Terahertz spectroscopy of explosives and drugs

Terahertz frequency radiation possesses a unique combination of desirable properties for noninvasive imaging and spectroscopy of materials. This includes the ability to obtain chemical and structural information about substances concealed within dry packaging, such as paper, plastics, and cardboard. As a result, the application of terahertz frequency spectroscopy for the sensing and identification of materials of security interest, such as explosives and, to a lesser extent, drugs-of-abuse, has caught the attention of a number of researchers and security agencies. We describe terahertz time-domain spectroscopy and examine the terahertz spectra of a wide range of drugs-of-abuse, pure explosives, and plastic explosives.

A. Giles Davies*, Andrew D. Burnett, Wenhui Fan, Edmund H. Linfield, and John E. Cunningham
School of Electronic and Electrical Engineering, University of Leeds, Leeds, LS2 9JT, UK
**E-mail: G.Davies@leeds.ac.uk*

The electromagnetic spectrum, illustrating the position of the terahertz (THz) frequency range with respect to the neighboring microwave/millimeter and mid-infrared (IR) regions of the spectrum, is shown in Fig. 1. The THz range is conventionally considered to be 0.3–10 THz ≡ 10–300 cm^{-1} ≡ 1–0.03 mm, although different authors adopt slightly different definitions. There has been considerable interest in this region of the spectrum for many decades now (see, for example, Nichols and Tear[1]), and a range of experimental techniques have been developed to access this frequency range. However, the exploitation of the THz range has been hindered by the limited number of convenient and suitable (in particular, coherent) radiation sources and detectors, which is related to the rather unique position of the THz region in the electromagnetic spectrum.

On the microwave side of the spectrum, it is difficult to fabricate electronic devices that operate at frequencies substantially above a few hundred gigahertz (although the output of such sources can be harmonically multiplied to the THz range). This is partly a result of the inherent need for very short carrier transit times in the active regions and is also a consequence of the low powers produced by devices, which must have small active areas to minimize their capacitance.

On the optical side of the spectrum, interband diode lasers have long been designed for operation at visible and near-IR frequencies. However, this concept, where light is generated by the radiative recombination of conduction band electrons with valence band holes across the bandgap of the active material, cannot be simply extended into the mid-IR or to longer wavelengths since suitable narrow bandgap semiconductors are not available.

ISSN:1369 7021 © Elsevier Ltd 2008

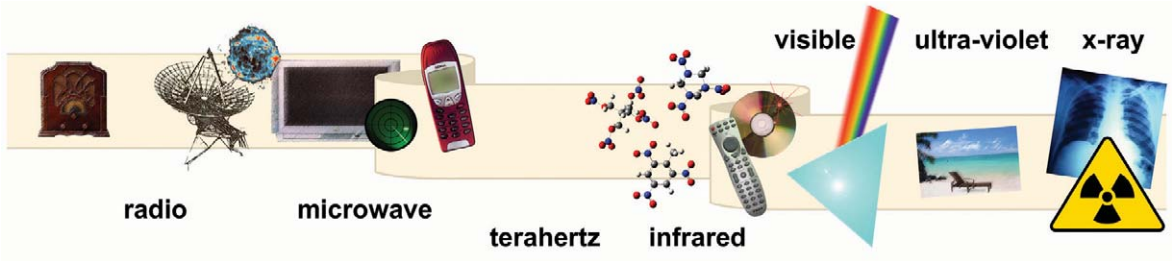

Fig. 1 Schematic representation of the electromagnetic spectrum illustrating the position of the THz frequency range.

Owing to these difficulties in fabricating solid-state THz sources, researchers have focused attention in recent years on all-optical techniques of producing THz radiation, employing visible/near-IR femtosecond pulsed lasers. This technique[2], developed in the mid-1980s, and the subsequent development of broadband THz time-domain spectroscopy (THz-TDS) and imaging systems (discussed below)[3], has led to the surge of international activity in this field.

It is with these coherent THz systems that many of the exciting prototype experiments have been undertaken, demonstrating the potential of THz radiation for imaging and spectroscopy in a number of application areas including those related to security screening. The recent development of a compact, solid-state THz semiconductor laser, the quantum cascade laser (QCL)[4], is set to revolutionize this field further. However, while these devices avoid the need for expensive and cumbersome femtosecond pulsed lasers, at present they do still require cryogenic cooling.

THz frequency imaging and spectroscopy

THz frequency radiation possesses a unique combination of desirable properties for nondestructive materials imaging and spectroscopy that has caught researchers' attention (see elsewhere for further reviews[5–7]). Many materials exhibit characteristic spectral features in the THz frequency range (particularly >1 THz), enabling THz spectroscopy to be used as a tool to uniquely identify chemical species. In addition to addressing intramolecular vibrational modes, THz spectroscopy can also excite intermolecular vibrations[8–10]. This gives THz spectroscopy the potential to provide both chemical and structural information. Indeed, THz-TDS has been shown to be a particularly sensitive technique for studying the structural dynamics of crystal forms, providing additional information for sample analysis. Furthermore, it is worth noting that THz-TDS can provide complementary spectral information to Raman spectroscopy, owing to the different selection rules governing IR and Raman transitions.

As an example, Fig. 2a shows a comparison between the absorption spectra of two chemically similar drugs-of-abuse: cocaine free base and cocaine hydrochloride (colloquially referred to as 'crack' and 'coke', respectively). Despite the relatively similar chemical structure, the THz frequency spectra are clearly distinct. For comparison, the Raman spectra of the same materials are shown over the same frequency range below (Fig. 2b).

THz-TDS is superior to other spectroscopic techniques in the far-IR range, such as Fourier transform infrared (FTIR) spectroscopy, as it is insensitive to the thermal background (and hence benefits from a high signal-to-noise ratio), and does not require a cryogenically cooled bolometer detector. THz-TDS also potentially allows both the absorption coefficient and the refractive index to be extracted directly without requiring a Kramers–Kronig analysis.

An attractive feature of THz spectroscopy is that this frequency radiation can be transmitted though many nonmetallic and nonpolar materials. This allows the possible spectral analysis of materials concealed within dry packaging, such as paper, plastics, cardboard, and, to a certain extent, clothing, enabling the imaging of concealed objects, such as metallic and ceramic knives, etc. This is clearly advantageous for security screening. For example, it is difficult with the well-established X-ray scanning techniques to distinguish between materials of similar density and elemental composition, and they provide no spectral information. However, for practical implementation of THz frequency stand-off detection systems, the progressive increase in atmospheric absorption >500 GHz, together with other factors such as scattering of radiation off clothing weaves, etc., need to be considered carefully.

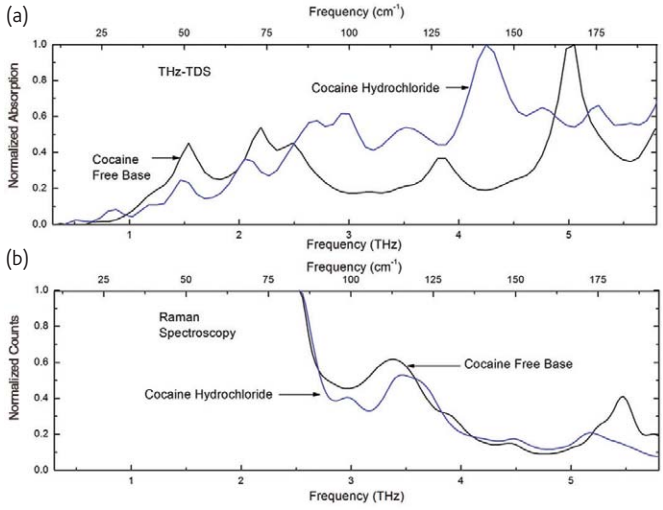

Fig. 2 Comparison between the far-IR spectra of polycrystalline cocaine free base and cocaine hydrochloride obtained using (a) THz-TDS and (b) Raman spectroscopy.

It has also been noted that THz frequency radiation has a relatively low photon energy in comparison with X-rays and is nonionizing, making it potentially more suitable for personnel scanning. Furthermore, the radiation power obtainable from typical THz-TDS systems is modest (<1 mW) and is not considered to pose a health risk[11,12], although as higher power QCL sources (greater than tens of milliwatts) become available, the implications of radiation exposure on the apparatus operators and personnel being scanned will need to be reviewed.

From a security screening point of view, there has been significant progress in recent years in the use of the millimeter wave/lower THz frequency range (50 GHz–1 THz), with some techniques now in operation at UK airports (see elsewhere for an excellent review[13]). Both active and passive imaging modalities have been investigated; the former involves the analysis of radiation directed at the target by an operator, while the latter relies on naturally occurring ambient radiation emitted by, or reflected off, the target. Fig. 3 shows an example of a passive outdoor image at 94 GHz with a spatial resolution of 3 mrad of an individual holding a metal knife concealed in a newspaper[13]. At 94 GHz, many dielectric materials such as clothing and paper are transparent. The reflection of radiation from the sky, which is very cold at this frequency, is apparent on the knife and the subject's head and shoulders, which results in these images having a very natural appearance. It is also noticeable that there is a reflection on the tarmac of the subject; tarmac is rough and a diffuse reflector at visible frequencies, but is smooth and provides specular reflection like a mirror at 94 GHz. Although there is little spectral information available over this frequency range, differences in the electromagnetic properties of skin, explosives, metal, etc., can allow the detection of weapons or concealed packages.

Fig. 3 A passive outdoor image of an individual holding a metal knife concealed in a newspaper obtained at 94 GHz. Although there is little spectral information available over this frequency range, differences in the electromagnetic properties of skin, explosives, metal, etc., can allow the detection of weapons or concealed packages[13]. (Courtesy of Roger Appleby, QinetiQ, UK.)

THz time-domain spectroscopy

Since the first use of femtosecond lasers to generate coherent THz frequency radiation[2], there has been a drive to develop higher power sources and systems of broader bandwidth[14,15]. A number of techniques have been explored, including bulk electro-optic rectification[16,17], surface field generation[18,19], and ultrafast switching of photoconductive emitters[20–24].

Of these different methods, photoconductive emitters have proved to be the most efficient technique for converting visible/near-IR pulses to THz radiation[23,24], and have been widely used for THz spectroscopy and imaging. In this technique, electron-hole pairs are generated in a semiconductor crystal using an above-bandgap femtosecond pulse, and these photoexcited carriers are then accelerated by an applied electric field. The photoexcited carriers constitute a transient current pulse, which emits THz radiation in accordance with Maxwell's equations[25,26].

Fig. 4 shows a typical experimental THz-TDS arrangement for coherent generation and detection of broad bandwidth THz radiation. Although the experimental details vary between different systems, in this example the emitter comprises two vacuum-evaporated NiCr/Au electrodes separated by a submillimeter-wide gap, fabricated on a 1-μm-thick, low-temperature-grown (LT) GaAs layer, itself grown on an undoped GaAs substrate. Suitably annealed LT-GaAs is an ideal material for this application, providing short photocarrier recombination lifetimes (a few hundred femtoseconds), together with both high resistivity (which allows high electric fields to be used) and high carrier mobility[27,28]. A bias voltage of around ±100 V, modulated at a few kilohertz, is applied across the emitter electrodes. A pulsed Ti:sapphire laser beam, typically of a few hundred milliwatts average power (~10–100 fs pulse width, 800 nm center wavelength) is focused onto the edge of one of the two electrodes, and THz pulses are generated as described above. In this arrangement, pulses with a usable bandwidth extending to ~3 THz are typically obtained.

In an alternative arrangement, the THz radiation is collected 'backwards' (in the direction of the reflected pump laser beam), with the result that the absorption and dispersion of the THz pulses in the GaAs substrate are minimized, leading to an enhanced bandwidth (~20–25 THz)[29]. The emitted THz pulses are collimated and focused onto the sample by a pair of parabolic mirrors; samples can be scanned across the focus to build up a two-dimensional image, with spectral information recorded at each pixel. The transmitted or reflected THz pulse is then collected and focused using another pair of parabolic mirrors onto a detector.

Coherent detection of the transmitted or reflected THz radiation can be achieved in a number of ways. Fig. 4 shows a technique based

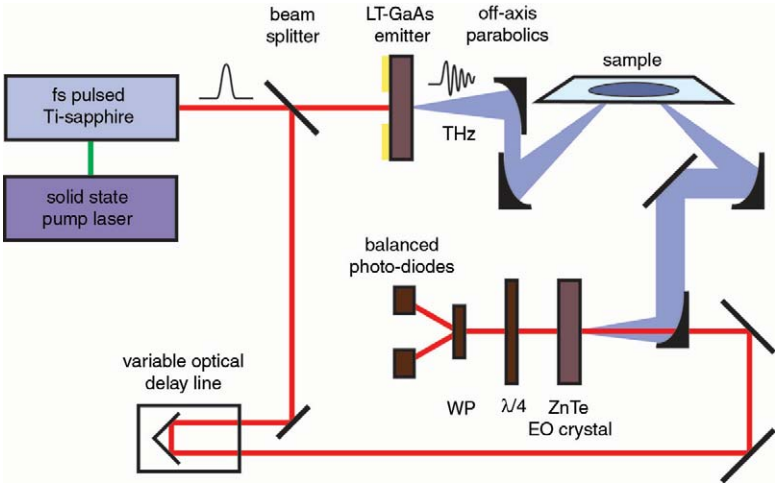

Fig. 4 Schematic of a THz-TDS system. In this example, the THz pulses are generated by a low-temperature-grown (LT)-GaAs photoconductive switch and subsequently detected, after reflection off the sample, by electro-optic sampling using a ZnTe electro-optic crystal. Although the diagram shows a sample being measured in a reflection geometry, the majority of studies employ a transmission arrangement. It is common to enclose the region in which the THz pulses propagate inside a vacuum-tight box, which can be evacuated or purged with dry nitrogen gas to reduce the effects of atmospheric absorption on the measurements.

on the ultrafast Pockels effect in which the THz beam is collected and focused onto an electro-optical sampling (EOS) detection crystal (e.g. (110) ZnTe)[30,31]. The THz field induces an instantaneous birefringence in the electro-optic medium, which is readily probed with a second visible/near-IR beam, initially split from the pump beam. The birefringence modulates the ellipticity of the probe beam, which is measured using a quarter waveplate (λ/4), a Wollaston polarization (WP) splitting prism, and two balanced photodiodes. Lock-in techniques can be used to measure the photodiode signal using the modulated bias field of the photoconductive emitter as a reference. Furthermore, by measuring this signal as a function of the time delay between the arrival of the THz and probe pulses at the electro-optic crystal using a variable delay line, the electric field of the THz pulse in the time domain can be obtained, and the Fourier transform gives the frequency spectrum of the THz radiation.

Fig. 5a shows a typical temporal THz waveform, with Fig. 5b showing the corresponding frequency spectrum[29]. The features at 5.2 THz and 8.0 THz in Fig. 5b are caused by absorptions in the ZnTe electro-optic detector crystal (transverse-optical (TO) phonon energy: 22 meV ≡ 5.3 THz) and the GaAs emitter (TO phonon energy: 33 meV ≡ 8.0 THz)[32], respectively. By replacing the ZnTe crystal with a second LT-GaAs photoconductive antenna, now acting as a gated receiver, the ZnTe phonon resonances are eliminated from the system and a smooth spectral distribution is obtained from 0.3 THz to 7.5 THz, ideal for spectroscopic applications[33].

Fig. 5b also shows the amplitude spectrum of the THz signal measured after transmission through a polytetrafluroethylene (PTFE) sample (lower trace). It is common practice to prepare compressed pellets of polycrystalline powdered samples, often incorporating a dilutant matrix material to reduce the THz attenuation in highly absorbing samples. Care needs to be taken to eliminate artifacts in the

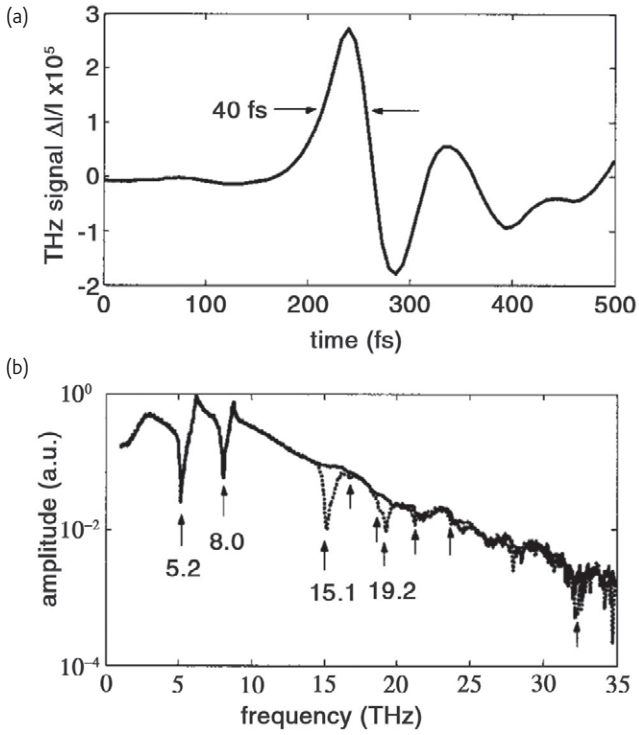

Fig. 5 (a) The temporal THz waveform and (b) its corresponding Fourier transform amplitude spectrum with (upper trace, solid line) no sample in the THz-TDS system and (lower trace, dotted line) a PTFE sample. (Reprinted with permission from[29]. © 2003 American Institute of Physics.)

measurements associated with such sample preparation[6]. Together with polyethylene (PE), PTFE is often used as a matrix material owing to its relatively high transparency and featureless spectrum. The spectrum in Fig. 5b demonstrates the useful bandwidth of this THz spectrometer; the observed spectral features are associated with CF_2 vibrations[34].

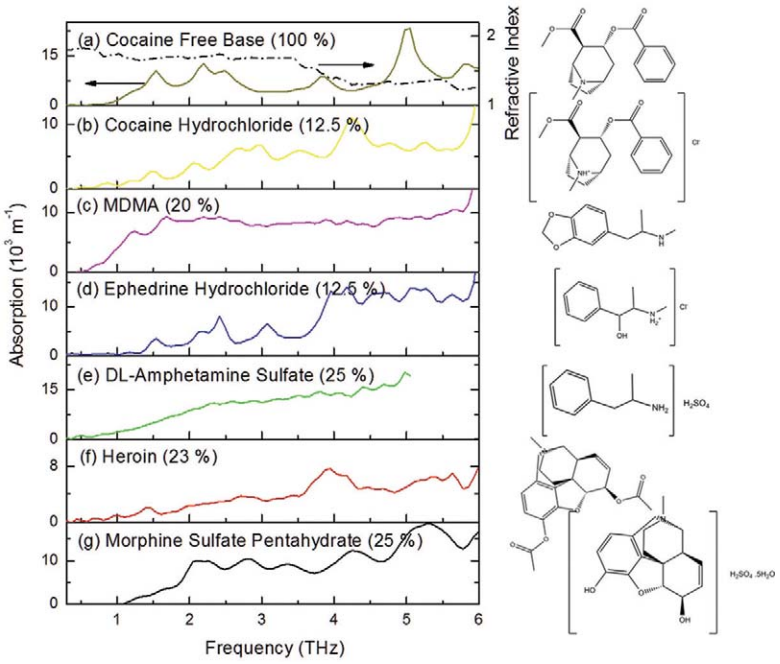

Fig. 6 THz absorption spectra of a range of common drugs-of-abuse. The samples are prepared as compressed pellets, diluting the pure drugs with PTFE powder; the percentage of drug (by weight) is indicated. A refractive index measurement is shown for cocaine free base, as an example. The cocaine free base and cocaine hydrochloride data is the same as shown in Fig. 2.

Drugs-of-abuse

A number of proscribed drugs-of-abuse, in particular amphetamine-type stimulants, have been investigated by THz-TDS and far-IR spectroscopy. Fig. 6 shows an overview of the THz-TDS spectra of seven drugs or drug precursors: (a) cocaine free base ('crack'); (b) cocaine hydrochloride ('coke'); (c) 3,4-methylenedioxy-N-methamphetamine (MDMA or 'ecstasy'); (d) ephedrine hydrochloride; (e) amphetamine sulfate; (f) diamorphine (heroin); and (g) morphine sulfate pentahydrate (morphine)[35,36]. The powdered samples of the pure chemicals were diluted with PTFE, as described in the caption, and compressed into pellets for measurement.

In real-world 'street' samples, of course, adulterants, dilutents ('cutting agents'), and impurities will contaminate the pure drugs-of-abuse, potentially complicating the spectral analysis. Unlike the various contaminants found in plastic explosives (as discussed later), these materials are often crystalline organic materials such as caffeine, lactose, or other pharmaceutical products, which will have spectral features in the THz range[36,37].

Cocaine

Cocaine is found in the leaves of the shrub *Erythroxylon coca* in the Andes. Once extracted from the leaf, it often arrives in the UK as cocaine hydrochloride. Cocaine stimulates dopamine receptors in the brain causing euphoria in a similar way to amphetamines. Cocaine hydrochloride ('coke') is often snorted or it can be heated with ether and bicarbonate of soda (known as 'cracking' or 'free-basing') to convert the drug back to its free base ('crack cocaine'), which is smoked. Figs. 6a and 6b show THz-TDS spectra of cocaine free base and cocaine hydrochloride, respectively. Clear, well-defined spectral features are observed up to 6 THz, with only one common peak at 1.54 THz. Cocaine hydrochloride has a considerably larger absorption coefficient probably owing to the large Cl counter ion, which increases the magnitude of the dipole moment and thus the change in dipole moment during a normal mode vibration.

As one potential advantage of THz-TDS is its ability to detect materials that have been deliberately concealed, Fig. 7a shows a series of THz-TDS spectra of cocaine free base behind a (single) disc of material cut from a number of different FedEx packages. Although the transmission is severely curtailed at ~1.5 THz through heavy cardboard, there is good transmission through the other packages allowing much, if not all, of the cocaine free base spectrum to be obtained.

Ecstasy, ephedrine hydrochloride, and amphetamine sulfate

MDMA or 'ecstasy' is a synthetic compound first patented in 1912 by Merck and used for medical purposes for a number of years. It is a popular club drug, often taken in tablet form, and is one of a large group of synthetic amphetamines, many of which have psychedelic properties. Amphetamines are structurally similar to adrenaline and noradrenaline, both natural chemicals in the body that increase heart and breathing rate, blood pressure, and metabolism in the so-called 'flight or fight' reaction (the natural reflex to fear or danger).

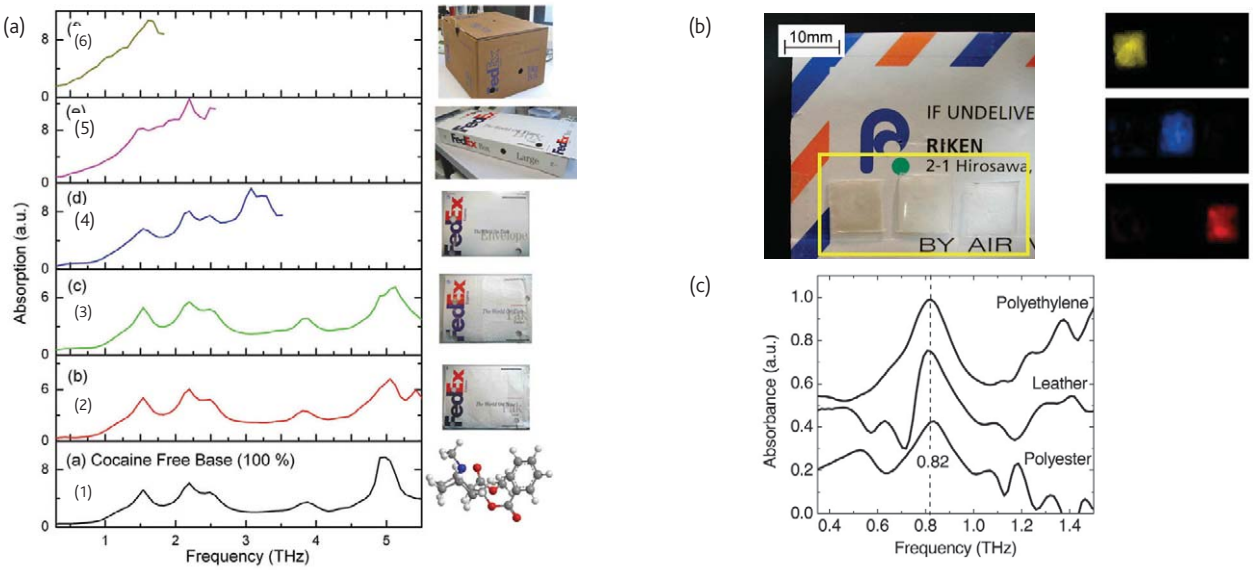

Fig. 7 (a) THz-TDS spectra of a compressed pellet of pure cocaine free base behind a (single) disc of material cut from a number of different Fed-Ex packages as illustrated. The lower panel shows the spectrum obtained with no covering material. The feature around 3.2 THz observed in panel (4) appears to be associated with the gloss finish on this package[36]. (b, left) Photograph showing three polythene bags containing, from left to right, MDMA, aspirin, and methamphetamine. The bags were placed inside the envelope shown prior to THz imaging. (b, right) Extracted spatial patterns of MDMA (yellow), aspirin (blue), and methamphetamine (red) using THz transmission spectroscopy. The three materials are clearly distinguished. (c) Absorption spectra of RDX obtained from diffuse reflection measurements through different covering materials. The RDX absorption peak at 0.82 THz can be clearly identified in each spectrum. (Part (b) reprinted with permission from[41] and part (c) from[62]. © 2003 and 2006 Optical Society of America, respectively.)

Investigations of amphetamine-type stimulants (methamphetamine, MDMA, and 4,5-methylenedioxy amphetamine)[38] demonstrate a clear spectral distinction between the three substances over the frequency range 0.2–2.5 THz. The spectral features seen at 1.24 THz, 1.71 THz, and 1.90 THz in Fig. 6c agree well with those observed in other studies[38–41]. Density functional theory (DFT) calculations of the vibrational modes of methamphetamine have also been carried out and found to agree well with the experimentally measured spectrum[39]. A further study has also shown that far-IR spectroscopy can distinguish between optical isomers and racemic mixtures of certain amphetamine-type stimulants[40]. Kawase *et al.*[41] have demonstrated the detection and discrimination of methamphetamine, MDMA, and aspirin, where the substances are hidden inside an envelope (Fig. 7b).

Ephedrine can be used as a precursor for amphetamine and other amphetamine derivatives such as ecstasy and, as such, its supply is often controlled. Fig. 6d shows a number of spectral features observed up to ~4 THz in a racemic mixture of ephedrine hydrochloride; above this frequency absorption peaks are difficult to define with poor signal-to-noise and broad features. Amphetamine sulfate has a relatively simple chemical structure and is also often used as the starting point in the synthesis of ecstasy. Amphetamine sulfate shows no observable absorption features over the THz frequency range (Fig. 6e); in fact, the samples prove highly absorbing for frequencies >3 THz (both for the racemic mixture shown here, and the pure D-enantiomer)[36].

It is interesting that the ephedrine spectrum shows a number of clearly defined absorption features despite having a similar molecular structure to MDMA and amphetamine sulfate, probably reflecting the significance that the solid-state crystal structure plays in determining the THz spectra of any compound.

Opiates

The opium poppy, *Papaver somniferum*, is the source of a number of opiates, which work in a similar way to the body's natural painkillers (endorphins and enkaphalins), blocking pain receptor sites in nerves and preventing pain signals reaching the brain. One of the most commonly known opiates is morphine (morphine sulfate pentahydrate), which is commonly used as a painkiller in hospitals. Morphine can be converted to diamorphine (heroin), one of the most important drugs-of-abuse internationally.

Heroin is formed by the acetylation of morphine using acetyl anhydride. During the reaction, a number of side reactions can occur, leading to the presence of a mixture of other alkaloids and opiates that can often provide information about a sample's provenance. THz-TDS spectroscopy shows characteristic absorption peaks at 1.42 THz and 3.94 THz (Fig. 6f). Fig. 6g shows the spectrum of the chemically similar morphine sulfate pentahydrate, which is distinct from that of both heroin and morphine hydrochloride[42].

Pharmaceuticals

In passing, it is worth noting that there has been significant interest in the use of THz-TDS for the study of pharmaceutical drug compounds. Each different polymorphic crystal form adopted by an organic

compound can have a set of unique physico-chemical properties, such as solubility, dissolution rate, or stability[43]. These properties are critical factors for the successful development and manufacture of pharmaceutical products, not least because they can profoundly influence pharmaceutical performance[44]. Techniques that allow the characterization and quantitative analysis of the various polymorphic forms are therefore of fundamental importance to the pharmaceutical industry, not only to verify production, but also for registration and patenting purposes.

In proving studies[45], the different polymorphic forms of theophylline, an oral bronchodilator in asthma therapy, have been characterized by THz-TDS over the frequency range 0.3–5.0 THz. Clear discrimination is observed between the spectra of the monohydrate form and an enantiotropic pair of anhydrous polymorphs. A number of other free-space THz-TDS demonstrations of pharmaceutical products and their polymorphs have been reported, including paracetamol (4-acetamidophenol) and aspirin (acetylsalicyclic acid)[41,46]; carbamazepine, enalapril maleate, indomethacin, and fenoprofen calcium[47,48]; and ranitidine hydrochloride[49]. The latter study shows that the products Zantac and Apo-ranitidine comprise different polymorphs, and furthermore demonstrate the applicability of THz-TDS to investigate pharmaceuticals in tablet form, as well as specially prepared samples. Furthermore, the fact that THz radiation can penetrate dry packaging materials potentially allows analysis of packaged products, which is of relevance as polymorphic states can change during storage[49].

Explosives

The potential for THz spectroscopy not only to provide chemical specificity, but also to penetrate packaging materials in a stand-off configuration, has led to international efforts to establish the application of this technique for the identification of explosives and improvised explosive devices. A wide range of explosive materials have been investigated by THz-TDS, including both pure explosive compounds and plastic explosives, the latter comprising an explosive compound or a mixture of explosives combined with a variety of plasticizers, desensitizers, dyes, waterproof coatings, and fabrics to aid storage and use. As with the cutting agents found in 'street' drugs-of-abuse, these adulterants may potentially have their own spectral signatures in the THz region, complicating or obscuring the analysis, although their presence may indicate the existence of a plastic explosive, and the 'recipe' may help determine the explosive's origin.

The pure explosive materials that have been studied using THz spectroscopy include ammonium nitrate[50,51], 2,4,6-trinitrotoluene (TNT) and its degradation product 2,4-dinitrotoluene[35,50–58], 1,3,5,7-tetranitro-1,3,5,7-tetrazocane (HMX)[50–52,55,56,58,59], 1,3,5-trinitroperhydro-1,3,5-triazine (RDX)[35,50–52,54–63], and 1,3-dinitrato-2,2-bis(nitratomethyl)propane (PETN)[35,51,54–59,63]. A comprehensive overview of the THz spectra of a wide range of explosive materials can be found elsewhere[51]. Studies of the plastic explosives Metabel (PETN-based)[55,63], SX2 (RDX-based)[35,55,57,63], C-4 (RDX-based)[52,60,64,65], PBX (predominantly containing HMX)[66], and Semtex-H (containing both RDX and PETN)[35,50,54,55,57,63] have also been reported. DFT calculations of the THz frequency vibrational modes of a number of these materials, including HMX[67], RDX[68], and PETN[69], have also been carried out (see also[51]).

Most investigations have focused on THz transmission spectroscopy, as this readily allows extraction of the absorption coefficient and refractive index of the sample, and the sample thickness/dilution can be optimized to maximize the measurement signal-to-noise ratio. However, there is growing interest in developing THz reflection spectroscopy geometries (both specular and diffuse), as this is the more natural arrangement for stand-off detection[61,62,65].

Fig. 8 shows examples of THz-TDS spectra for RDX and PETN, together with the plastic explosives Metabel, Semtex, and SX2[35,54,57,63]. As with the drugs-of-abuse, the pure materials were diluted with PTFE and compressed into a pellet for these measurements. The plastic explosives were cut into a slice (<1 mm thick) with a scalpel and measured without further preparation.

RDX and PETN

RDX is a white crystalline powder that is found in a large number of military explosive compositions and is considered to be one of the most stable and powerful high explosives. RDX comprises an unusual six-membered heterocyclic ring comprising three nitrogen and three methylene groups, with a nitrite group attached to each of the nitrogen atoms in the ring. This high nitrogen and oxygen content contributes to making RDX an excellent explosive.

A typical THz-TDS spectrum of RDX is shown in Fig. 8a, and a number of characteristic absorption features can be observed. The sensing of RDX through covering materials such as plastic, leather and cotton has been investigated[51]; the same has been done using a reflection geometry[62]. In both cases the spectral features of RDX (and in particular, the absorption peak at 0.8 THz) can be identified (Fig. 7c).

PETN is more sensitive to shock or friction than RDX (or TNT) and is also an extremely powerful explosive. It is often used in blasting caps, detonating chord, or as a booster, although it is also found as a large constituent of some plastic explosives such as Semtex. PETN is a coarse, white powder that is often transported damp to desensitize it. Fig. 8a shows a THz-TDS spectra of PETN in which several clear absorption features can be observed.

Plastic explosives

Most explosive materials are not used in their pure molecular crystalline form, but are mixed with other agents to make plastic explosives. The range and relative concentration of these ingredients vary from sample to sample, although the explosive compounds generally dominate the composition. Figs. 8b–8d show the

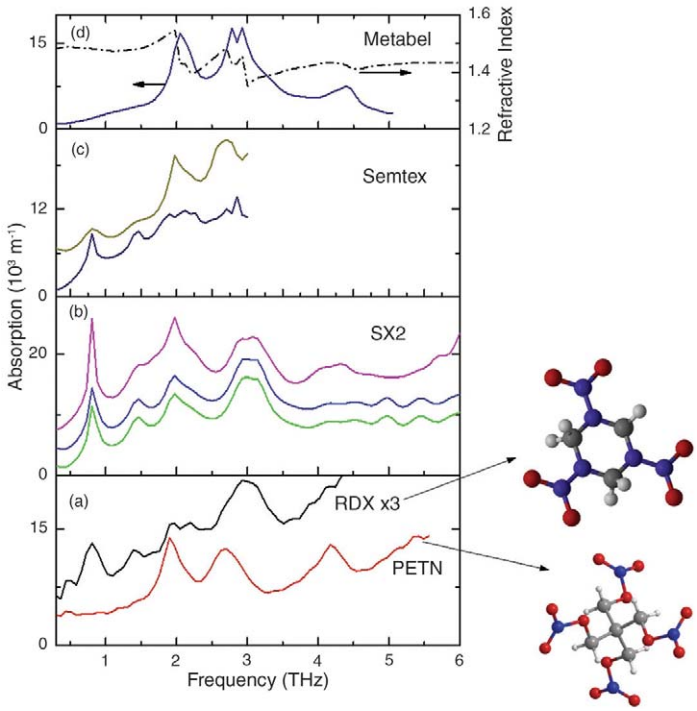

Fig. 8 THz absorption spectra of a range of common explosives. The pure explosive samples (PETN and RDX) were diluted with PTFE powder to a 30:70 (explosive: PTFE) ratio by weight, and compressed into pellets. The plastic explosives (Metabel, Semtex, and SX2) were cut into thin slices and measured without further preparation. In the case of Semtex and SX2, several spectra are shown, each arising from a different sample batch. A refractive index measurement is shown for Metabel, as an example.

transmission spectra of SX2 (a British military explosive, similar to C-4), Semtex, and Metabel, allowing a comparison with the spectra of their constituent explosives, PETN and RDX. Metabel shares three corresponding absorption features with PETN and little obvious contribution from any other compound present (Fig. 8d). Similarly, there is a clear correspondence between the features observed in the spectra of SX2 and its constituent explosive RDX (Fig. 8b). Semtex contains both RDX and PETN and, although the ratio of the two explosives varies, the total explosive content normally comprises around 90%[70]. Comparison of the spectrum of Semtex with those of its component explosives shows a correlation in a number of peaks, e.g. a peak at 0.81 THz can be seen in the spectra of both Semtex and RDX (Fig. 8c). Other peaks in the Semtex spectrum have a contribution from vibrational modes of both RDX and PETN, as well as a number of other components.

The spectra of the plastic explosives shown in Fig. 8 are dominated by the signatures arising from their constituent explosives. The THz transmission spectra of a range of the dyes, antioxidants, and rubber binders likely to be found in plastic explosives have been explicitly measured to establish whether they could confuse a THz-TDS measurement[67]. In general, data collected so far suggest that most of the nonexplosive components are transparent to THz radiation, making spectral analysis of plastic explosives much simpler than the complex drug mixtures discussed above.

Ammonium nitrate

Ammonium nitrate has a high proportion of oxygen and nitrogen for its weight, and is thus an excellent oxidizer for other compounds (fuel, sugar) and, in high purity, can act as an explosive itself. It is easy to obtain, being a common component of fertilizer. Ammonium nitrate shows an extremely high absorption in the THz frequency range, with negligible transmission above 2.5 THz and no defining spectral features (not shown)[50,51]. Although THz spectroscopy would be unable to identify the presence of ammonium nitrate chemically, its high absorption could plausibly enable it to be located in a THz frequency image[6].

Conclusions and future outlook

We have seen that THz frequency spectroscopy can be used to identify and discriminate explosives and drugs-of-abuse on the basis of their characteristic fingerprint spectra, not only as pure crystalline materials, but also in real-world 'street' forms. However, the majority of these studies have been carried out in laboratory environments, and the transfer of this technology into the field for security screening applications is not straightforward and will inevitably require further development in the underlying technology (an excellent discussion of some of the challenges is provided elsewhere[6]).

It is undoubtedly true that a cheap, compact, tunable, continuous-wave THz source with implementation of commensurate detectors

would revolutionize this field. The development of THz frequency QCL technology (with the demonstration of its use in imaging at distances greater than 25 m)[71] offers many exciting future possibilities, despite the current need for cryogenic cooling and the limited tuning range.

In parallel with such system developments, however, there remains the need to improve our understanding of the underlying interactions of THz frequency radiation with matter; for example, the ability to discriminate between scattering and absorption phenomena, or to be able to model the spectra observed from common crystalline materials realistically[9,10]. The latter is particularly challenging because of the large number of atoms that need to be considered to predict spectral features arising from the combination of inter- and intra-atomic vibrations.

Time will only tell whether such developments will lead to THz imaging systems being exploited routinely in everyday life and, in particular, in a security context. But whatever happens, this is a fascinating region of the electromagnetic spectrum and there is still much to be done to understand and exploit its potential. mt

Acknowledgments

We are grateful to the following colleagues for stimulating discussions: Roger Appleby, Howard Cummins, Paul Dean, Howell Edwards, Michael Hargreaves, Matthew Hogbin, Richard Jenkinson, John Kendrick, Tasmin Munshi, Ian Scowen, Garth Shilstone, Prashanth Upadhya, and John Whyte. We are grateful for the support of the UK Engineering and Physical Sciences Research Council, the Research Councils UK Basic Technology Program, the European Commission program TeraNova, HM Government Communications Centre, the Defence Science and Technology Laboratory, HM Revenue and Customs, the Home Office Science Development Branch, and the Forensic Science Service.

REFERENCES

1. Nichols, E. J., and Tear, J. D., *Astrophys. J.* (1927) **61**, 17
2. Auston, D. H., *et al.*, *Appl. Phys. Lett.* (1984) **45**, 284
3. See, for example, Nuss, M. C., and Orenstein, J., In *Millimeter and Submillimeter Wave Spectroscopy of Solids*, Grüner, G., (ed.), Springer, Berlin, (1998), and references therein
4. Köhler, R., *et al.*, *Nature* (2002) **417**, 156
5. Siegel, P. H., *IEEE Trans. Microwave Theory Tech.* (2002) **50**, 910
6. Federici, J. F., *et al.*, *Semicond. Sci. Technol.* (2005) **20**, S266
7. Woolard, D. L., *et al.*, *Proc. IEEE* (2005) **93**, 1722
8. Walther, M., *et al.*, *Chem. Phys.* (2003) **288**, 261
9. Uhd Jepsen, P., and Clark, S. J., *Chem. Phys. Lett.* (2007) **442**, 275
10. Allis, D. G., *et al.*, *Chem. Phys. Lett.* (2007) **440**, 203
11. Berry, E., *et al.*, *J. Laser Appl.* (2003) **15**, 192
12. Berry, E., *J. Biol. Phys.* (2003) **29**, 263
13. Appleby, R., and Wallace, H. B., *IEEE Trans. Antennas Prop.* (2007) **55**, 2944
14. Ferguson, B., and Zhang, X.-C., *Nat. Mater.* (2002) **1**, 26
15. Beard, M. C., *et al.*, *J. Phys. Chem. B* (2002) **106**, 7146
16. Wu, Q., and Zhang, X.-C., *Appl. Phys. Lett.* (1997) **71**, 1285
17. Kaindl, R. A., *et al.*, *Appl. Phys. Lett.* (1990) **75**, 1060
18. Dekorsy, T., *et al.*, *Phys. Rev. B* (1996) **53**, 4005
19. Johnston, M. B., *et al.*, *Phys. Rev. B* (2002) **65**, 165301
20. Krökel, D., *et al.*, *Appl. Phys. Lett.* (1989) **54**, 1046
21. Keil, U. D., and Dykaar, D. R., *Appl. Phys. Lett.* (1992) **61**, 1504
22. Katzenellenbogen, N., and Grischkowsky, D., *Appl. Phys. Lett.* (1991) **58**, 222
23. Brener, I., *et al.*, *Opt. Lett.* (1996) **21**, 1924
24. Zhao, G., *et al.*, *Rev. Sci. Instrum.* (2002) **73**, 1715
25. Castro-Camus, E., *et al.*, *Phys. Rev. B* (2005) **71**, 195301
26. Upadhya, P. C., *et al.*, *Opt. Lett.* (2007) **32**, 2297
27. Zhang, K., and Miller, D. L., *J. Electron. Mater.* (1993) **22**, 1433
28. Gregory, I. S., *et al.*, *Appl. Phys. Lett.* (2003) **83**, 4199
29. Shen, Y.-C., *et al.*, *Appl. Phys. Lett.* (2003) **83**, 3117
30. Wu, Q., and Zhang, X.-C., *Appl. Phys. Lett.* (1997) **70**, 1784
31. Leitenstorfer, A., *et al.*, *Appl. Phys. Lett.* (1999) **74**, 1516
32. Tani, M., *et al.*, *J. Appl. Phys.* (1998) **83**, 2473
33. Shen, Y.-C., *et al.*, *Appl. Phys. Lett.* (2004) **85**, 164
34. Gruger, A., *et al.*, *Vib. Spectrosc.* (2001) **26**, 215
35. Burnett, A., *et al.*, *Proc. SPIE* (2006) **6402**, 64020B
36. Burnett, A., *et al.*, unpublished data
37. See, for example, http://webbook.nist.gov/chemistry/thz-ir
38. Sun, J.-H., *et al.*, *Chin. Phys. Lett.* (2005) **22**, 3176
39. Ning, L., *et al.*, *Opt. Express* (2005) **13**, 6750
40. Kishi, T., *et al.*, Joint 30th International Conference on Infrared and Millimeter Waves and 13th International Conference on Terahertz Electronics, (2005), 184
41. Kawase, K., *et al.*, *Opt. Express* (2003) **11**, 2549
42. Fischer, B., *et al.*, *Semicond. Sci. Technol.* (2005) **20**, S246
43. See, for example, Henck, J.-O., *et al.*, *J. Am. Chem. Soc.* (2001) **123**, 1834
44. Morissette, S. L., *et al.*, *Adv. Drug Delivery Rev.* (2004) **56**, 275
45. Upadhya, P. C., *et al.*, *Spectrosc. Lett.* (2006) **39**, 215
46. Taday, P. F., *Philos. Trans. R. Soc. London, Ser. A* (2004) **362**, 351
47. Strachan, C. J., *et al.*, *Chem. Phys. Lett.* (2004) **390**, 20
48. Strachan, C. J., *et al.*, *J. Pharm. Sci.* (2005) **94**, 837
49. Taday, P. F., *et al.*, *J. Pharm. Sci.* (2003) **92**, 831
50. Cook, D. J., *et al.*, *Proc. SPIE* (2004), **5354**, 55
51. Chen, J., *et al.*, *Opt. Express* (2007) **15**, 12060
52. Agrawal, V., *et al.*, IEEE 6th International Conference on Terahertz Electronics, (1998), 34
53. Chen, Y., *et al.*, *Chem. Phys. Lett.* (2004) **400**, 357
54. Burnett, A., *et al.*, *Proc. SPIE* (2006) **6120**, 61200M
55. Lo, T., *et al.*, *Vib. Spectrosc.* (2006) **42**, 243
56. Fitch, M. J., *et al.*, *Chem. Phys. Lett.* (2007) **443**, 284
57. Fan, W.-H., *et al.*, *Appl. Spectrosc.* (2007) **61**, 638
58. Leahy-Hoppa, M. R., *et al.*, *Chem. Phys. Lett.* (2007) **434**, 227
59. Barber, J., *et al.*, *J. Phys. Chem. A* (2005) **109**, 3501
60. Choi, M. K., *et al.*, *Philos. Trans. R. Soc. London, Ser. A* (2004) **362**, 337
61. Shen, Y.-C., *et al.*, *Appl. Phys. Lett.* (2005) **86**, 241116
62. Liu, H.-B., *et al.*, *Opt. Express* (2006) **14**, 415
63. Burnett, A., *et al.*, *Proc. SPIE* (2007) **6549**, 654905
64. Yamamoto, K., *et al.*, *Jpn. J. Appl. Phys.* (2004) **43**, L414
65. Sengupta, A., *et al.*, *Proc. SPIE* (2005) **6120**, 61200A
66. Funk, D. J., *et al.*, *Appl. Spectrosc.* (2004) **58**, 428
67. Allis, D. G., *et al.*, *J. Phys. Chem. A* (2006) **110**, 1951
68. Rice, B. M., and Chabalowski, C. F., *J. Phys. Chem. A* (1997) **101**, 8720
69. Allis, D. G., and Korter, T. M., *ChemPhysChem* (2006) **7**, 2398
70. Hobbs, J. R., Proceedings of the 4th International Symposium on Analysis and Detection of Explosives, Jerusalem, Israel, (1992), 409
71. Lee, A. W. M., *et al.*, *Appl. Phys. Lett.* (2006) **89**, 141125